Calculation of Magnetic Couplings in Hydrogen-Bonded Cu(II) Complexes Using Density Functional Theory

ARTICLE *in* THE JOURNAL OF PHYSICAL CHEMISTRY A · MARCH 2012

Impact Factor: 2.69 · DOI: 10.1021/jp300618v · Source: PubMed

2 AUTHORS:

Nuno A. G. Bandeira
ICIQ Institute of Chemical Research of Catal…
25 PUBLICATIONS **153** CITATIONS
SEE PROFILE

Boris Le Guennic
Université de Rennes 1
137 PUBLICATIONS **2,367** CITATIONS
SEE PROFILE

THE JOURNAL OF PHYSICAL CHEMISTRY A

Article

pubs.acs.org/JPCA

Calculation of Magnetic Couplings in Hydrogen-Bonded Cu(II) Complexes Using Density Functional Theory

Nuno A. G. Bandeira[†,‡] and Boris Le Guennic*[,†,§]

[†]Université de Lyon, CNRS, Institut de Chimie de Lyon, Ecole Normale Supérieure de Lyon, 15, Parvis René Descartes, BP7000, 69342 Lyon Cedex 07, France

[‡]C8 - Fac. Ciências, Univ. de Lisboa, Campo Grande 1749-016 Lisbon Portugal

[§]Institut des Sciences Chimiques de Rennes, UMR 6226 CNRS-Université de Rennes 1, 35042 Rennes Cedex, France

ABSTRACT: The performance of recent density functionals for computation of molecular magnetic coupling constants (J) in hydrogen-bonded systems is evaluated. A survey of six Cu(II) dinuclear complexes is considered. The global accuracy trend is GGAs < meta-GGAs < hybrid-GGAs ≈ hybrid meta-GGAs. Hybrid meta-GGAs do not generally provide any improvement over well-established hybrid functionals such as B3LYP. It is also seen that spin projection values agree best with experiment if one uses functionals that either have large quantities of exact exchange such as B2PLYP or functionals with long-range Coulomb screening such as CAM-B3LYP or LC-ωPBE, thus suggesting that these provide a description that is free from self-interaction errors.

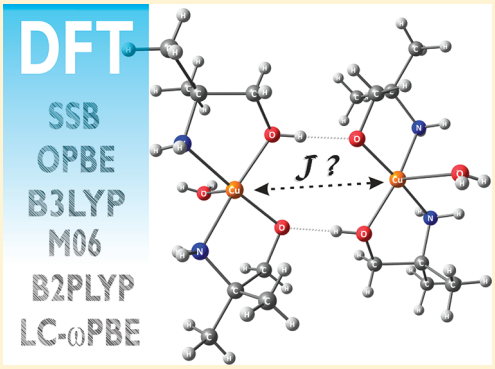

I. INTRODUCTION

Hydrogen bonds[1,2] play a major role in biology or chemistry since these weak bonds are at the forefront of fundamental research in the fields of crystal engineering,[3] DNA structuration,[4] biochemical reactions,[5] or spin transition.[6] In molecular magnetism,[7,8] whereas magnetic exchange couplings between metal ions are realized usually through coordination bonds, the possibility of observing magnetic exchange through weak supramolecular interactions such as hydrogen bridges has been reported for complexes based on diverse metal centers such as V(IV),[9] Cr(III),[10−13] Fe(II),[14] Fe(III),[15] Co(II),[16,17] Ni(II),[17,18] and mixed-metal binuclear complexes.[19] Moreover, numerous examples of H-bonded Cu(II) dinuclear complexes have been already described experimentally[20−30] and addressed theoretically.[31−34]

The most common form to assess the magnetic properties of a molecule is based on the phenomenological Heisenberg−Dirac−Van Vleck (HDVV) Hamiltonian

$$\hat{H} = -\sum_{i<j} J_{ij}\hat{S}_i\cdot\hat{S}_j \qquad (1)$$

in which J_{ij} is the magnetic coupling constant between magnetic centers i and j and $\hat{S}_i$ the spin operator on center i. In the simplest case of a d^1 or d^9 binuclear complex, J is given by the singlet−triplet spin states energy difference $J = E_S - E_T$ and the Hamiltonian takes the simple form $\hat{H} = -J\hat{S}_1\cdot\hat{S}_2$.

The goal of this paper is to test up-to-date density functionals with regard to their description of the J constant in the specific case of hydrogen-bonded magnetic systems. The difficulty in accurately placing the hydrogen atoms with common X-ray crystallography leads one to pose the question of whether or not to optimize the atomic positions of the hydrogen atoms. This is what we plan to address further in this paper.

II. BACKGROUND

Computation of J can be achieved using accurate multireference wave function approaches such as CASPT2[35,36] or multireference CI (DDCI,[37,38] SORCI[39]), with some—but increasingly less—limitation in the size of the studied complex (see refs 40−44 for recent applications). When dealing with through-H magnetic interactions, DDCI calculations have shown also to be a valuable tool to quantitatively evaluate the role of weak bonds in the exchange interactions by selectively turning on specific mechanisms.[34] A second approach consists of dealing with the electron density through density functional theory (DFT).[45] In the present contribution, we thus focus on application of DFT to calculation of J in H-bonded Cu(II) dinuclear units taking a close look at the performance of recent density functionals.

Although DFT is a single-reference method, it can be applied to this problem using either the broken symmetry (BS) approach[46−49] or the more recently proposed "constrained DFT".[50,51] To date, the former is better known and has been more widely used and developed.[52−55] Whereas the triplet state can be represented with a single determinant $|a_g^{\uparrow}a_u^{\uparrow}|$ in which a_g and a_u molecular orbitals correspond to the gerade (i.e., in-phase) and ungerade (out of phase) combinations of the

Received: January 18, 2012
Revised: March 8, 2012
Published: March 8, 2012

magnetic orbitals on the metal centers, the same cannot be said for the open-shell singlet which typically is a linear combination of two determinants $1/\sqrt{2} \times (|a_g^{\uparrow} a_u^{\downarrow}| - |a_g^{\downarrow} a_u^{\uparrow}|)$. Within the BS approach, this problem can be circumvented by calculating the energy of just one determinant, the broken symmetry determinant, for instance, $|a_g^{\uparrow} a_u^{\downarrow}|$, followed by the use of a spin projection (SP) formula to extract the value of J such as the one proposed by Nishino et al.[56]

$$J = \frac{2(E_{BS} - E_T)}{\left\langle \hat{S}_T^2 \right\rangle - \left\langle \hat{S}_{BS}^2 \right\rangle} \cong 2(E_{BS} - E_T) \tag{2}$$

where E_{BS} and E_T are the energies of the broken symmetry and triplet states, respectively. $\langle \hat{S}_T^2 \rangle$ and $\langle \hat{S}_{BS}^2 \rangle$ are the mean values of the spin-squared operator of each of the calculated states, typically 2.0 and 1.0 for a two-electron problem.

While use of spin projection is theoretically well grounded,[57−61] some authors[62−64] have noted that using a nonspin-projected (NSP) formula

$$J = E_{BS} - E_T \tag{3}$$

in which the energy of the singlet state (E_S) is approximated by the broken symmetry state E_{BS}, does provide better agreement with experimental values of J, in particular, if the popular global-hybrid B3LYP[65] functional is used. The reason that is adduced by the holders of this strategy is the self-interaction error[66,67] (SIE), which is present in common density functionals and leads to mimicking of some static correlation. In this contribution, rather than taking sides in this debate, we will simply list both approaches and draw our conclusions from the numerical trends.

For a pertinent benchmark, the set of functionals has to comprise both classical generalized gradient approximation (GGA) or global-hybrid functionals as well as more recently developed functionals including meta-GGA, hybrid meta-GGA, range-separated hybrid (RSH), and double-hybrid functionals. Even if it is established that GGA functionals often overestimate the antiferromagnetic character of a magnetic coupling, i.e., favor the lowest spin state, three recently proposed GGA functionals were selected. Indeed, particular effort has been made in benchmarking functionals for the general case of spin states in mononuclear complexes. Recent achievements by Swart et al.[68,69] have shown that the combination of the OPTx exchange with Perdew's PBE correlation functionals (OPBE) provides a computationally tractable methodology for handling of these spin states, particularly for iron complexes that are fair models of biomolecules. An extension of the OPBE functional later came into fruition with the SSB functional[70] based on an arithmetical switch between PBEx, which provides considerable accuracy in reaction barriers and all round energetics, and OPTx, which accounts well for spin crossover phenomena. Since only its dispersion-corrected variant is implemented in the ADF program suite (which we mainly used in this study, see computational details), SSB-D will be considered as the most suitable candidate in the pure GGA class of functionals. Let us note that the dispersion correction itself will be of no special use since no optimization of the molecular geometries was carried out.

Among the global-hybrid functionals, B3LYP has proven to be effective in computing J values (with the NSP formula) for a large variety of polynuclear complexes.[64,71,72] To test the importance of the exact exchange admixture, we used the variant of B3LYP functional called B3LYP* which incorporates 15% of exact exchange instead of 20%.[75,76] This functional was proposed by Reiher et al.[73,74] as a more accurate functional for the spin energetics of transition metal complexes. The recently developed hybrid meta-GGA M06 functional[75,76] has recently been used concomitantly by Ruiz[77] and Valero et al.[78] to compute the magnetic coupling constant J in a variety of well-known complexes. Unfortunately, it was reported that the performance of this functional remains roughly identical to that of standard global-hybrid GGAs such as B3LYP or PBE0.[79] Among other hybrid meta-GGAs, the recent work by Jensen[80] provided the conclusion that TPSSh which includes 10% of exact exchange "achieves an unprecedented mean absolute error [...] in spin transition energies" closely followed by the nonhybrid M06-L. However, Vancoillie et al.[81] found that M06-L and M06 both tend to overstabilize the high-spin forms, and the former was deemed more accurate in the authors' test set.

The long-range-corrected LC-ωPBE functional[82] has also recently shown promising performance to describe dissociative phenomena and hydrogen bonds,[82,83] as well as magnetic phenomena.[84−86] Its screened Hartree−Fock exchange makes it appropriate to treat electronic localization effects and affords a correct description of asymptotic behavior of the exchange potential. As the screening value $\omega \to 0$ the functional will approach the form of PBE0, whereas if $\omega \to \infty$ the functional will approach the form of pure PBE. In LC-ωPBE this value of ω is empirically set to 0.4 bohr^{-1}, although Phillips et al.[85] recommend the value 0.5 bohr^{-1} specifically for calculation and analysis of magnetic systems. We will use the default value of ω because the added accuracy reported by Phillips is not too significant (15% better agreement with experimental values). Another long-range-corrected functional CAM-B3LYP by Handy et al.[87] built on the well-known B3LYP hybrid functional has also been chosen. The asymptotic behavior of the Coulomb attenuated method (CAM) is slightly different and more general than the LC approach in that the functional need not fluctuate between a pure and a hybrid form but rather just different values of the exact exchange component ($0.19 \leq a_x \leq 0.65$). In a thorough analysis of the performance of long-range-corrected functionals in calculation of J for a large set of transition metal binuclear complexes, it is conclusive that the best procedure remains the use of B3LYP combined with a NSP procedure but that some long-range-corrected functionals, in particular, LC-ωPBE, provide good results if the SP procedure is used.[86,88]

Double-hybrid functionals[89] are functionals where in addition to using exact exchange (a_x = 0.53 in B2PLYP) a Møller−Plesset-type perturbation part is included, at second order, on the correlation functional expression (with c = 0.27 in B2PLYP). For spin states, Ye and Neese[90] found that although reasonably accurate, B2PLYP tends to be more biased in favor of high-spin states. Schwabe and Grimme[91] tested the performance of some double-hybrid functionals including B2PLYP on calculation of J for a few copper complexes. It was unambiguously noticed that in the SP framework results improve with respect to those obtained with hybrid functionals. Let us mention that the applicability of B2PLYP is also suitable[92] to hydrogen-bonded systems since it incorporates some long-range effects in the perturbative treatment of the dynamical correlation functional.

The recent spin-flip time-dependent DFT (SF-TDDFT) methodology[93−96] should also be mentioned. It has been implemented in a few software packages such as QChem[97] or

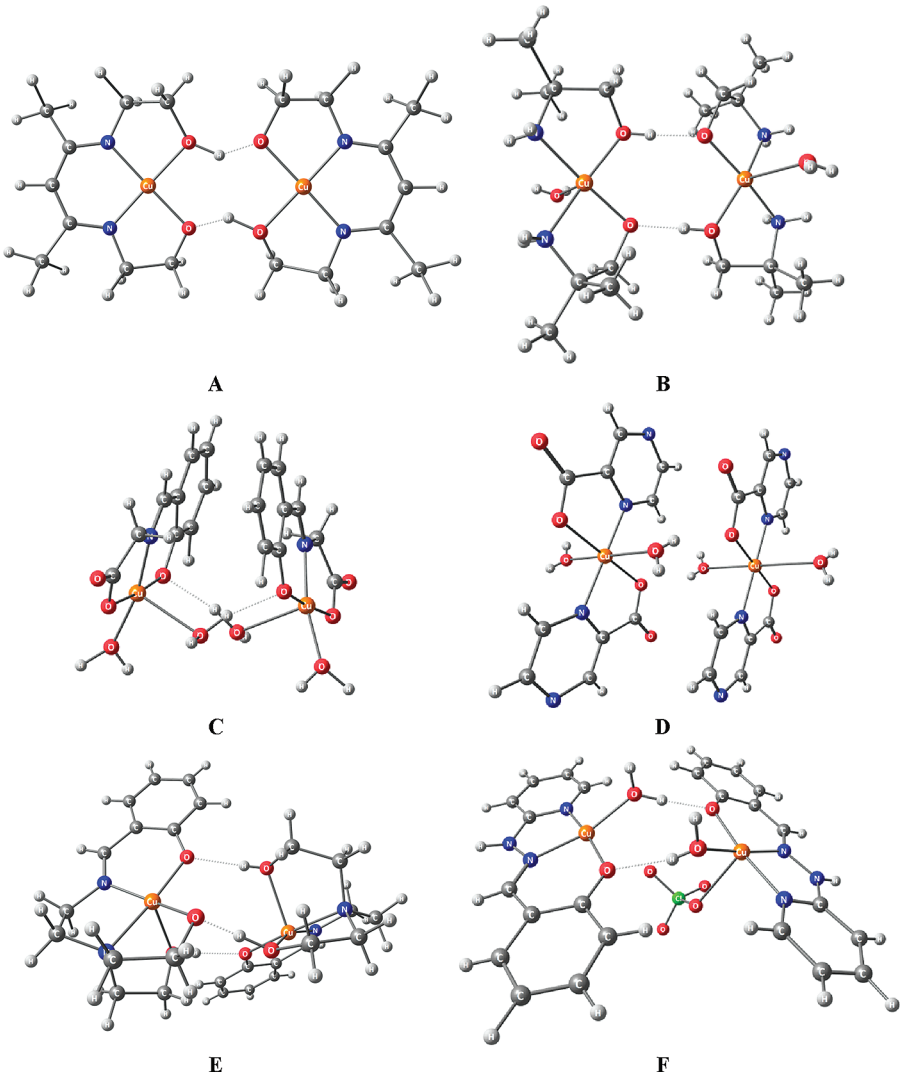

Figure 1. Representation of the six studied binuclear Cu(II) molecules with the respective CCDC ref codes **A** = HEAICU10,[115] **B** = AETCUB,[116] **C** = SAGLAC,[21] **D** = BEYRAY01,[117] **E** = ODALAG,[24] and **F** = FUTCON.[26] Cu···Cu distances are as follows: 4.989 (**A**), 4.935 (**B**), 5.253 (**C**), 5.439 (**D**), 4.614 (**E**), and 4.890 Å (**F**).

ADF and has the advantage of taking into account the several Slater determinants present in the singlet wave function if one takes the triplet M_s = +1 (↑↑) determinant as the departure state, thus discarding the spin projection controversy. Since there is the possibility of obtaining a negative excitation, the Tamm−Dancoff approximation should be employed, although it should be noted that the meaningful[98] energy difference should be between the M_s = 0 components (↑↓ ± ↑↓) of the triplet and the singlet states that the spin-flip calculation yields rather than the direct M_s = +1 → M_s = 0 excitation value. The first published application of the SF-TDDFT methodology to calculation of magnetic coupling constants has been published very recently by Valero et al.[98] and Zhekova et al.,[99,100] while other areas have also been explored.[101,102] The main result was that the values yielded by the SF-TDDFT approach in the test sets closely resemble those of BS with SP, which is unfortunate since they are usually double the experimental values. The method outperforms this classic broken symmetry approach if the amount of Hartree−Fock exchange is kept at a high value (typically 40%) in B1PW91- or B1LYP-type functionals. For the sake of completeness we will employ this methodology associated with the B3LYP40 functional (c = 0.4) to this work.

III. METHODOLOGY

The 2010.01 version of the Amsterdam Density Functional (ADF) program[103] was used for all but calculations regarding the LC-ωPBE, CAM-B3LYP, and B2PLYP functionals for which the Gaussian09[104] program suite was used. Single-point energy evaluations were performed on the published X-ray diffraction crystal structures. ADF calculations were carried out with triple-ζ Slater-type basis sets with an additional polarization function (TZP). Integration accuracy was set to 6.0. Spin-flip time-dependent DFT calculations[93,94,105] were performed using the Tamm−Dancoff approximation[106] and the adiabatic local density approximation (ALDA) to the exchange correlation kernel.

The LC-ωPBE, CAM-B3LYP, and ω-B97X calculations used the Ahlrichs' triple-ζ valence (TZVP) basis set[107] for all atoms. B2PLYP calculations used the Ahlrichs' split valence (SVP) basis set[108] with automatic generation of fit functions ('Auto' keyword). No symmetry constraints were used throughout the whole series of calculations. Potential energy surface scans were performed for the triplet states, and each optimized point

dx.doi.org/10.1021/jp300618v | J. Phys. Chem. A 2012, 116, 3465−3473

Table 1. Magnetic Couplings (J, in cm^{-1}) with the Corresponding Mean Average Error (MAE)[c] and Mean Relative Error (MAPE)[d] from Experiment[a]

DFT method	A	B	C	D	E	F	MAE (cm^{-1})	MAPE (%)
PBE	−327	−91	−0.4	0.0	−23	−55	51	143
	−655	*−181*	*−0.8*	*0.0*	*−46*	*−111*	*133*	*319*
OPBE	−313	−78	−0.4	0.0	−21	−48	45	128
	−625	*−157*	*−0.8*	*0.0*	*−42*	*−95*	*121*	*289*
SSB-D	−269	−71	−0.4	0.0	−15	−45	35	103
	−538	*−141*	*−0.8*	*−0.1*	*−31*	*−89*	*101*	*239*
M06-L	−177	−50	−0.2	+0.1	−9	−31	19	59
	−354	*−99*	*−0.4*	*+0.2*	*−18*	*−62*	*57*	*133*
B3LYP	−80	−25	+0.1	−0.2	−4	−12	12	70
	−160	*−49*	*+0.2*	*−0.4*	*−8*	*−24*	*14*	*73*
B3LYP*	−109	−32	−0.1	0.0	−6	−17	10	48
	−218	*−65*	*−0.2*	*0.0*	*−11*	*−34*	*25*	*73*
M06	−78	−27	−0.6	−0.2	−4	−11	13	65
	−157	*−53*	*−1.2*	*−0.4*	*−9*	*−21*	*14*	*61*
TPSSh	−122	−37	+0.4	+1.0	−6	−20	11	72
	−244	*−74*	*+0.8*	*+2.0*	*−13*	*−39*	*30*	*172*
LC-ωPBE	−44	−15	+6.3	−4.6	−14	−6	24	390
	−88	*−39*	*+12.6*	*−9.2*	*−28*	*−12*	*17*	*713*
ω-B97X	−44	−14	−0.1	−0.1	−2	−6	22	81
	−88	*−29*	*−0.2*	*−0.1*	*−4*	*−12*	*10*	*63*
CAM-B3LYP	−49	−16	−0.1	0.0	−2	−6	20	78
	−98	*−32*	*−0.2*	*−0.1*	*−5*	*−13*	*8*	*58*
B2PLYP	−39	−12	0.0	−21.5	−2	−11	26[e]	71[e]
	−79	*−24*	*−0.1*	*−43.0*	*−4*	*−22*	*14*[e]	*49*[e]
SF-TDB3LYP	−175	−54	−0.2	−0.1	−20	−47	23	108
SF-TDB3LYP40	−56	−18	−0.1	−0.2	−11	−16	17	76
experiment[b]	**−96**	**−70**	**−2.2**	**+0.3**	−7	**−20**		

[a]In italics are the SP values. [b]Experimental magnetic couplings taken from the literature (**A** = HEAICU10,[115] **B** = AETCUB,[116] **C** = SAGLAC,[21] **D** = BEYRAY01,[117] **E** = ODALAG,[24] and **F** = FUTCON[26]). [c]MAE = $(1/n)\sum_i|J_{i,\mathrm{calcd}} - J_{i,\mathrm{exp}}|$. [d]MAPE = $(1/n)\sum_i(((|J_{i,\mathrm{calcd}} - J_{i,\mathrm{exp}}|)/(|J_{i,\mathrm{exp}}|)) \times 100)$. [e]Does not take **D** into account.

underwent a broken symmetry single-point run to compute the value of J.

IV. RESULTS AND DISCUSSION

Six Cu(II) binuclear complexes were selected (see Figure 1), partly following the selection of Desplanches et al.[31] Two more recent systems were also considered in the tested panel.[24,26] Our intention was to collect a variety of complexes exhibiting diverse topologies of hydrogen bridges and different magnitudes of magnetic coupling. We are unaware of the existence of a strongly ferromagnetic Cu(II) system with a hydrogen-bond exchange pathway. Therefore, complex **D** will serve as a test for both accuracy and precision in the density functional sample due to its minute value of J. For the sake of completeness, one shall mention that all these previous studies[31,24,26] already include calculations with the B3LYP functional. No comparison with other functionals was realized at that stage.

The overall results are given in Table 1 together with experimental values and mean average errors (MAE). The trend for decreasing error is GGAs < meta-GGAs < hybrid-GGAs ≈ hybrid-meta-GGAs, which is in line with findings from the literature pertaining to magnetism in covalently bonded systems.[78,88,109] Results obtained with 'pure' density functionals (with no exact exchange) better agree with the experimental values if spin projection is not used. This is the case for PBE (GGA) right across to M06-L (meta-GGA), the latter being slightly more accurate than the former. However, all are generally a long way off from the experimental values for every system, with the exception of complexes **C** and **D** for which the correct sign of the small J values is reproduced. With OPBE, the J values generally only yield a marginal improvement over PBE. One would expect SSB-D to provide an intermediate answer between the latter two since it is conceived to switch between PBE and OPBE as a function of the reduced density gradient. Obviously, this is not the case since the values of J with SSB-D are usually in better agreement with experiment than either PBE or OPBE. This is more visible in systems **A** and **B** for which a stark improvement in their J values is observed. This can be due to the fact that either Swart[70] used a simplified version of the PBE correlation functional which might have some influence or the exchange part of SSB employs a semiempirical correction initially proposed by Keal and Tozer.[110] The latter is more likely to be the cause of numerical improvement since exchange plays an important role in the description of magnetic systems.

Not surprisingly, inclusion of exact exchange in the density functionals provides a much better agreement with experimental values of J relative to pure functionals whether one uses SP or not. The amount of exact exchange (B3LYP vs B3LYP*) also yields a discernible change in the J values. For example, with B3LYP, the 'best' calculated J value for **A** is -80 cm^{-1} (NSP), almost off by 20 cm^{-1} from the experimental value (-96 cm^{-1}), whereas with B3LYP*, this same value of J turns out to be slightly better by comparison (-109 cm^{-1}). This underpins the well-known behavior whereby higher percentages

dx.doi.org/10.1021/jp300618v | J. Phys. Chem. A 2012, 116, 3465−3473

of Hartree−Fock (HF) exchange favor high-spin states and lower percentages favor low spin forms. Higher HF exchange naturally implies less spin delocalization, and consequently, the NSP values of B3LYP* better agree with experimental ones (see Table 1). However, it is tentative to speculate that B3LYP* might be an altogether better formulation of B3LYP.

It is also noticeable that the double-hybrid B2PLYP functional provides a better agreement with experiment if spin projection is taken into account. This is not surprising since this functional contains a large amount of exact exchange, therefore overstabilizing the singlet states. Let us note how close are the B2PLYP (SP) J values (apart from J_D) and the NSP J values obtained with B3LYP. A large anomaly comes up for complex **D** for which B2PLYP (and to some extent LC-ωPBE) fails to predict this short singlet−triplet gap, whereas other functionals have no problem doing so. It does not seem to be a bias problem since for **C** the J value is equally small but the error is of the same magnitude as the remaining functionals. It should not be due to the perturbative treatment of the correlation part since the value of J_D without it (i.e., the B2LYP functional) is equal to −20 cm^{-1} (J_D = −22 cm^{-1} with B2PLYP), so consequently, the P-LYP correlation correction yields only a small change in J. The possible cause of this large numerical anomaly could be the size of the basis set which was chosen to be split valence (SVP) for reasons of computational tractability since the PT2 treatment requires a great deal of machine memory.

If we focus our attention on the largest numerical values of magnetic coupling constants, i.e., complexes **A**, **B**, and **F** with experimental J values of −96, −70, and −20 cm^{-1}, respectively, one sees that either the SP or the NSP formulas can provide, randomly, the best numerical answer where some of the hybrid functionals are concerned, while it is generally known that in classical (i.e., covalent) magnetic systems NSP data better reproduce[77,78,91] the experimental J values. As an example, B3LYP produces a J value for **A** of −80 cm^{-1} (NSP), which is relatively close to the experimental one (−96 cm^{-1}). However, for complex **B**, J is closer to its experimental value if one uses the SP formula. With M06, as with B3LYP, the answer in favor of either SP or NSP is not clear. Applying the NSP formula generally only provides marginal improvement on the value of their MAE. However, TPSSh and B3LYP* present a much clearer agreement with experiment if the NSP procedure is used. For instance, TPSSh yields an MAE = 11 (NSP) vs 30 (SP). This may be down to the minute amount of exact exchange in both functionals.

Use of the range-separated functional LC-ωPBE does not overall provide any noticeable improvement over other hybrid functionals. This is in agreement with the recent findings of Phillips et al.,[85] who concluded no noticeable improvement of the space partitioning across short- and long-range regions. Only the absolute weight of the exact exchange in the functional was deemed important. Moreover, LC-ωPBE incorrectly predicts **C** to be largely ferromagnetic, a noticeable failure for this functional. Apart from **D** and **E**, this functional overestimates ferromagnetism in our test set. In his recent study,[88] Ruiz observed an interesting improvement with long-range-corrected functionals if a SP approach is used. In our set of H-bonded systems, such a trend does not clearly emerge. However, with CAM-B3LYP a significant agreement with experiment is seen for SP values of J. Indeed, it has the lowest MAE of all the functionals even though the improvement is only marginal over the NSP values of B3LYP*. It would seem

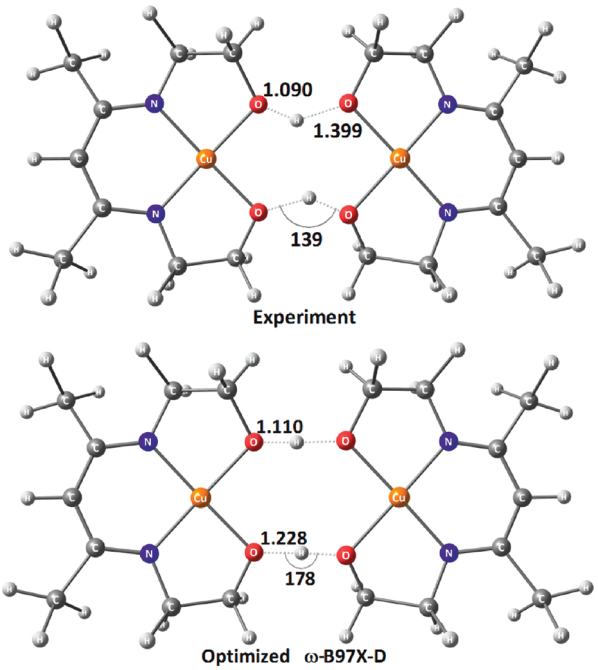

Figure 2. Structural parameters of the crystallographic structure (top) and partially optimized structure (bottom) of complex **A**.

that CAM-B3LYP is the spin-projected counterpart of B3LYP* and worthy of attention of computational practitioners wishing to employ spin projection in their calculations.

The spin-flip time-dependent B3LYP (SF-TDB3LYP) results show that the J value is overestimated, the only exception being model **B** which is just 20 cm^{-1} away from the experimental value. MAE and MAPE values are higher for SF-TDB3LYP than for the BS values whether in SP or NSP form. However, modifying the exact exchange amount to c = 0.4 (SF-TDB3LYP40) as done in the literature[98] we notice that the MAE and MAPE values improve significantly, attaining a similar accuracy to that of B3LYP. Unfortunately, SF-TDB3LYP40 fails to improve on the already well-established broken symmetry technique with B3LYP which is by far the most popular approach in the literature.

Since the position of the hydrogen atoms is quite often not accurately established in X-ray crystallography, it is interesting to evaluate to what degree the magnetic coupling changes as a function of the H-atom optimization or the Cu−Cu distance. An initial discussion to this effect was already made by Desplanches et al.,[31] who analyzed the evolution of the calculated (B3LYP) J value through a rigid scan of either the O···O distance or the coordination planes of the two monomers. We shall focus on model **A** hereafter and on one functional (ω-B97X) adding Grimme's dispersion correction[111] for better optimization. Addition of the dispersion term will help provide a better description of the hydrogen bond if the functional is lacking it. For this complex, ref 31 mentions only a minor change (2 cm^{-1}) in J upon moving the hydrogen atoms to the center of the O···O vector. On the other hand, Le Guennic et al.[32] found that the coupling constant is greatly sensitive to the O−H···O angle. For the experimental geometry, the result obtained with the ω-B97X functional is J(SP) = −88 cm^{-1} (see Table 1). If only the bridging hydrogen atoms are allowed to relax while keeping the rest of the structure rigid we obtain instead a value J(SP) = −134 cm^{-1}. This finding contradicts the one mentioned in ref 31 since the J

dx.doi.org/10.1021/jp300618v | J. Phys. Chem. A 2012, 116, 3465−3473

value is considerably changed as the hydrogen-bond path becomes a straight line. Indeed, the structural parameters of the hydrogen atoms vary considerably for the H-bond-relaxed structure with ω-B97X-D (Figure 2). These structural changes enhance the magnetic coupling with this particular functional.

In order to understand how geometry relaxation influences this kind of magnetic coupling we undertook another series of calculations on model **A** with the same functional. We fixed all the Cu−N and Cu−O distances (Scheme 1) while keeping the

Scheme 1. Structural Parameters Varied in the Stepwise Optimizations Varying d^a

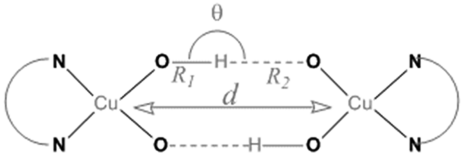

[a]The angle θ is also optimized. In grey are the optimized parts and in dark the constrained bonds.

remaining atoms free (distances, bond and dihedral angles) and performed a relaxed scan of the Cu−Cu distance d starting from the experimental value of 4.99 Å. The results are summarized in Figure 3. We observe a shallow parabolic

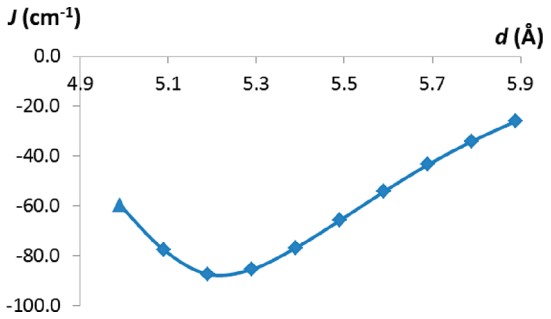

Figure 3. Variation of the coupling constant J(SP) (cm^{-1}) as a function of the metal−metal distance (d, Angstroms) for the complex **A**.

behavior with a minimum value of J(SP) = −88 cm^{-1} at 5.19 Å Cu−Cu separation. Whereas with all the atoms frozen except the bridging hydrogen atoms we obtained a large coupling constant of −134 cm^{-1}, in this instance we obtain more modest values. One thus observes a qualitative difference in the curve with the one calculated by Desplanches et al.[31] in which there was no inflection point but the novel aspect of our calculation is the relaxation at every constrained inter-metal distance. If we monitor the spin density of the bridging hydrogen atoms in the broken symmetry states (Figure 4) we notice also another inflection point at d = 5.09 Å. This leads to the conclusion that there is a point at which the spin density of the molecule starts to increase, and this can be directly related to the overlap population of the 2p orbitals of the oxygen with the 1s of hydrogen, which can be expressed by the Mayer−Mulliken bond order (MBO).[112,113] Usually, but not invariably, bond strengths are directly proportional to internuclear distances. A strong O···H hydrogen bond on one side of the molecule corresponds to a slightly weaker O−H bond on the other side since the overlap population is shared between both oxygen atoms. This doubtless has consequences in the sign of the spin

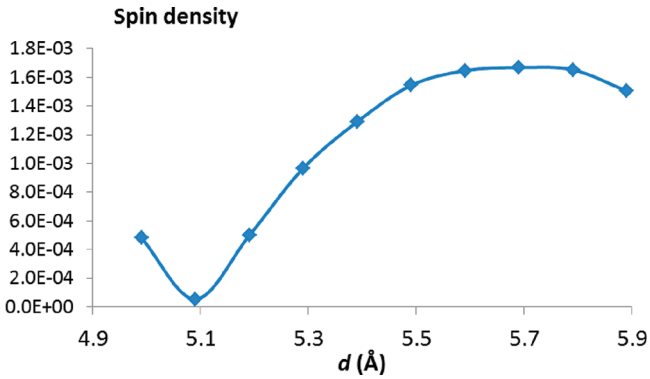

Figure 4. Variation of the average spin density of the bridging H atoms in the broken symmetry state as a function of the metal−metal distance (d, Angstroms) for the complex **A**.

densities of the bridging atomic centers. If we observe the data presented in Table 2 (see also Scheme 1) one notices that the

Table 2. Average Structural Parameters of the Relaxed Scan and Mayer Bond Orders (MBO) as a Function of Intermetal Distance (d, Angstroms)

d (Å)	R_1 (Å)	MBO (R_1)	R_2 (Å)	MBO (R_2)
4.99	1.055	0.679	1.409	0.266
5.09	1.047	0.696	1.443	0.242
5.19	1.036	0.716	1.495	0.214
5.29	1.025	0.737	1.567	0.181
5.39	1.014	0.759	1.653	0.150
5.49	1.004	0.778	1.747	0.123
5.59	0.997	0.796	1.847	0.103
5.69	0.990	0.812	1.954	0.087
5.79	0.985	0.825	2.062	0.075
5.89	0.981	0.835	2.175	0.066

strength of the hydrogen bond decreases with increasing Cu···Cu distance, since the MBO for the O···H fragment decreases from 0.266 all the way to almost zero. Note that since the Cu−O−H angles are not constrained, the sum $R_1 + R_2$ does not remain constant.

One may also note that the minima of J and the spin density of the bridging hydrogen atoms as a function of the intercopper distance do not strictly match, and the minimum in Figure 3 is shallower than the one in Figure 4, which is surely a sign that other processes may be at stake in this magnetostructural change.

Hydrogen bonds do not just provide a structural motif for the spin coupling, but they also play a part in the overall wave function. Since the coupling takes place via a spin delocalization mechanism[114] one can explain the behavior of the curve in Figure 4 by taking into account two limiting situations (Scheme 2): one with equal OH bonds (**2**) in which case the bridging hydrogen atom must have zero spin density since it sits at the center of two regions of opposing spin, and the other in which

Scheme 2. Spin Alignment of the Broken Symmetry States As a Function of the O−H Distance

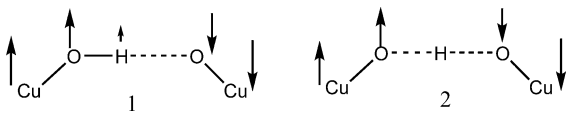

dx.doi.org/10.1021/jp300618v | J. Phys. Chem. A 2012, 116, 3465−3473

the hydrogen atom is sufficiently bound to the oxygen atom to allow it to align its spin density according to the central copper ion (**1**). O−H−O bonds with equal O−H lengths (**2**) are never reached, but one comes closer to this idealized case at the beginning of the structural change. If we examine the results in Table 2, the $R_2 - R_1$ difference is just 0.4 Å at d = 5.09 Å whereas this difference increases along the reaction path reaching 1.2 Å at d = 5.89 Å.

This demonstrates, if it was necessary, that the crystallographic placement of the hydrogen atoms influences the computational value of the magnetic coupling constants where the exchange path involves hydrogen bonding. This is a corollary to the statement that hydrogen bonds have an actual magnetic role through the electron density.

V. CONCLUSION

DFT calculation of magnetic couplings in hydrogen-bonded complexes was examined with present-day density functionals. While functionals that do not contain exact exchange can be specifically used without spin projection, their accuracy, even with pure meta-GGAs, leave a lot to be desired sometimes in error by as much as 80 cm^{-1}. Better overall accuracy is obtained with hybrid functionals; the best of them are B3LYP* and TPSSh followed by M06 all without spin projection corrections. For the long-range-corrected CAM-B3LYP functional, spin projection seems to produce results with the least deviation to experiment. A similar trend is found with B2PLYP, but its accuracy over the previous functional is not worth the extra computational effort of the perturbation treatment. Meta-GGA hybrid functionals such as TPSSh and M06 do not deliver any noticeable improvement over the traditional GGA hybrid B3LYP, in line with similar findings[77,78] for coordinate transition metal dimers.

Moreover, the structural parameters of complex **A** were investigated with particular relevance given to the position and spin densities of the bridging hydrogen atoms. It was found that the magnetic coupling of the dimer complex is highly dependent on the structural parameters of the bridging hydrogen, and furthermore, the in-plane increase of the Cu···Cu distance yields a parabolic dependence of the J(SP) values. The complex dimer **A** shows a dominant spin delocalization mechanism, and examination of the spin densities present in the O−H···O bridge shows how the bridging bond provides the essential tipping point through which the magnetic coupling takes place.

AUTHOR INFORMATION

Corresponding Author

*E-mail: boris.leguennic@univ-rennes1.fr.

Notes

The authors declare no competing financial interest.

ACKNOWLEDGMENTS

This work was developed within the "fdp magnets" project (ANR-07-JCJC-0045-0). The authors thank the Pôle Scientifique de Modélisation Numérique (PSMN) at ENS de Lyon for computing facilities.

REFERENCES

(1) Latimer, W. M.; Rodebush, W. H. *J. Am. Chem. Soc.* **1920**, *42*, 1419.
(2) Pauling, L. *The Nature of the Chemical Bond*, 3rd ed.; Cornell University Press: New York, 1960.
(3) Aakeroy, C. B.; Champness, N. R.; Janiak, C. *CrystEngComm* **2010**, *12*, 22.
(4) Szyc, Ł.; Yang, M.; Nibbering, E. T. J.; Elsaesser, T. *Angew. Chem., Int. Ed. Engl.* **2010**, *49*, 3598.
(5) Denisov, E. T.; Denisova, T. G. *Russ. Chem. Rev.* **2009**, *78*, 1047.
(6) Guionneau, P.; Marchivie, M.; Bravic, G.; Létard, J.-F.; Chasseau, D. In *Spin Crossover in Transition Metal Compounds II*; Springer-Verlag: Berlin, 2004; Vol. *234*, p 97.
(7) Kahn, O. *Molecular Magnetism*; Wiley-VCH: New York, 1993.
(8) Mrozinski, J. *Coord. Chem. Rev.* **2005**, *249*, 2534.
(9) Papoutsakis, D.; Ichimura, A. S.; Young, J. V. G.; Jackson, J. E.; Nocera, D. G. *Dalton Trans.* **2004**, 224.
(10) Ardon, M.; Bino, A.; Michelsen, K.; Pedersen, E. *J. Am. Chem. Soc.* **1987**, *109*, 5855.
(11) Bossek, U.; Haselhorst, G.; Ross, S.; Wieghardt, K.; Nuber, B. *J. Chem. Soc., Dalton Trans.* **1994**, 2041.
(12) Bossek, U.; Wieghardt, K.; Nuber, B.; Weiss, J. *Angew. Chem., Int. Ed. Engl.* **1990**, *29*, 1055.
(13) Goodson, P. A.; Glerup, J.; Hodgson, D. J.; Michelsen, K.; Rychlewska, U. *Inorg. Chem.* **1994**, *33*, 359.
(14) Garge, P.; Chikate, R.; Padhye, S.; Savariault, J. M.; De Loth, P.; Tuchagues, J. P. *Inorg. Chem.* **1990**, *29*, 3315.
(15) De Munno, G.; Ventura, W.; Viau, G.; Lloret, F.; Faus, J.; Julve, M. *Inorg. Chem.* **1998**, *37*, 1458.
(16) Zurowska, B.; Mrozinski, J.; Ciunik, Z.; Ochocki, J. *J. Mol. Struct.* **2006**, *791*, 98.
(17) Ma, Y.; Cheng, A.-L.; Gao, E.-Q. *Dalton Trans.* **2010**, *39*, 3521.
(18) Figgis, B. N.; Kennedy, B. J.; Murray, K. S.; Reynolds, P. A.; Wright, S. *Aust. J. Chem.* **1982**, *35*, 1807.
(19) Zhang, D.; Wang, H.; Chen, Y.; Ni, Z.-H.; Tian, L.; Jiang, J. *Inorg. Chem.* **2009**, *48*, 11215.
(20) Vasková, Z.; Moncol, J.; Korabik, M.; Valigura, D.; Svorec, J.; Lis, T.; Valko, M.; Melník, M. *Polyhedron* **2010**, *29*, 154.
(21) Estes, W. E.; Hatfield, W. E. *Inorg. Chem.* **1978**, *17*, 3226.
(22) Muhonen, H. *Inorg. Chem.* **1986**, *25*, 4692.
(23) Moreno, J. M.; Ruiz, J.; Dominguez-Vera, J. M.; Colacio, E. *Inorg. Chim. Acta* **1993**, *208*, 111.
(24) Plass, W.; Pohlmann, A.; Rautengarten, J. *Angew. Chem., Int. Ed. Engl.* **2001**, *40*, 4207.
(25) Valigura, D.; Moncol, J.; Korabik, M.; Pucekova, Z.; Lis, T.; Mrozinski, J.; Melnik, M. *Eur. J. Inorg. Chem.* **2006**, 3813.
(26) Tang, J.; Sánchez Costa, J.; Golobič, A.; Kozlečvar, B.; Robertazzi, A.; Vargiu, A. V.; Gamez, P.; Reedijk, J. *Inorg. Chem.* **2009**, *48*, 5473.
(27) Biswas, C.; Drew, M. G. B.; Asthana, S.; Desplanches, C.; Ghosh, A. *J. Mol. Struct.* **2010**, *965*, 39.
(28) Okazawa, A.; Ishida, T. *Chem. Phys. Lett.* **2009**, *480*, 198.
(29) Talukder, P.; Sen, S.; Mitra, S.; Dahlenberg, L.; Desplanches, C.; Sutter, J.-P. *Eur. J. Inorg. Chem.* **2006**, *2006*, 329.
(30) Nelson, D. J.; Cervanteslee, F.; Terhaar, L. W. *Abstr. Pap. Am. Chem. Soc.* **1992**, *204*, 236.
(31) Desplanches, C.; Ruiz, E.; Rodriguez-Fortea, A.; Alvarez, S. *J. Am. Chem. Soc.* **2002**, *124*, 5197.
(32) Le Guennic, B.; Ben Amor, N.; Maynau, D.; Robert, V. *J. Chem. Theory Comput.* **2009**, *5*, 1506.
(33) Nepveu, F.; Gehring, S.; Walz, L. *Chem. Phys. Lett.* **1986**, *128*, 300.
(34) Costa, J. S.; Bandeira, N. A. G.; Le Guennic, B.; Robert, V.; Gamez, P.; Chastanet, G.; Ortiz-Frade, L.; Gasque, L. *Inorg. Chem.* **2011**, *50*, 5696.
(35) Andersson, K.; Malmqvist, P. A.; Roos, B. O.; Sadlej, A. J.; Wolinski, K. *J. Phys. Chem.* **1990**, *94*, 5483.
(36) Andersson, K.; Malmqvist, P.-A.; Roos, B. O. *J. Chem. Phys.* **1992**, *96*, 1218.
(37) Miralles, J.; Daudey, J.-P.; Caballol, R. *Chem. Phys. Lett.* **1992**, *198*, 555.

(38) Miralles, J.; Castell, O.; Caballol, R.; Malrieu, J.-P. *Chem. Phys.* **1993**, *172*, 33.
(39) Neese, F.; Petrenko, T.; Ganyushin, D.; Olbrich, G. *Coord. Chem. Rev.* **2007**, *251*, 288.
(40) Queralt, N.; Taratiel, D.; de Graaf, C.; Caballol, R.; Cimiraglia, R.; Angeli, C. *J. Comput. Chem.* **2008**, *29*, 994.
(41) Le Guennic, B.; Robert, V. *C. R. Chim.* **2008**, *11*, 650.
(42) Negodaev, I.; de Graaf, C.; Caballol, R. *J. Phys. Chem. A* **2010**, *114*, 7553.
(43) Negodaev, I.; Queralt, N.; Caballol, R.; de Graaf, C. *Chem. Phys.* **2011**, *379*, 109.
(44) Rota, J.-B.; Calzado, C. J.; Train, C.; Robert, V. *J. Chem. Phys.* **2010**, *132*, 154702.
(45) Kohn, W.; Sham, L. J. *Phys. Rev.* **1965**, *140*, A1133.
(46) Noodleman, L. *J. Chem. Phys.* **1981**, *74*, 5737.
(47) Noodleman, L.; Norman, J. G. *J. Chem. Phys.* **1979**, *70*, 4903.
(48) Yamaguchi, K.; Tsunekawa, T.; Toyoda, Y.; Fueno, T. *Chem. Phys. Lett.* **1988**, *143*, 371.
(49) Yamanaka, S.; Kawakami, T.; Nagao, H.; Yamaguchi, K. *Chem. Phys. Lett.* **1994**, *231*, 25.
(50) Wu, Q.; Van Voorhis, T. *Phys. Rev. A* **2005**, *72*, 024502.
(51) Rudra, I.; Wu, Q.; van Voorhis, T. *J. Chem. Phys.* **2006**, *124*, 024103.
(52) Blanchet-Boiteux, C.; Mouesca, J.-M. *J. Phys. Chem. A* **2000**, *104*, 2091.
(53) Mouesca, J.-M. *J. Chem. Phys.* **2000**, *113*, 10505.
(54) Onofrio, N.; Mouesca, J.-M. *Inorg. Chem.* **2011**, *50*, 5577.
(55) Onofrio, N.; Mouesca, J.-M. *J. Phys. Chem. A* **2010**, *114*, 6149.
(56) Nishino, M.; Yoshioka, Y.; Yamaguchi, K. *Chem. Phys. Lett.* **1998**, *297*, 51.
(57) Illas, F.; de P. R. Moreira, I.; de Graaf, C.; Barone, V. *Theor. Chem. Acc.* **2000**, *104*, 265.
(58) Adamo, C.; Barone, V.; Bencini, A.; Broer, R.; Filatov, M.; Harrison, N. M.; Illas, F.; Malrieu, J.-P.; de P. R. Moreira, I. *J. Chem. Phys.* **2006**, *124*, 107101.
(59) Illas, F.; de P. R. Moreira, I.; Bofill, J. M.; Filatov, M. *Phys. Rev. B* **2004**, *70*, 132414.
(60) Caballol, R.; Castell, O.; Illas, F.; de P. R. Moreira, I.; Malrieu, J.-P. *J. Phys. Chem. A* **1997**, *101*, 7860.
(61) de P. R. Moreira, I.; Illas, F. *Phys. Chem. Chem. Phys.* **2006**, *8*, 1645.
(62) Ruiz, E.; Cano, J.; Alvarez, S.; Alemany, P. *Int. J. Quantum Chem.* **1999**, *20*, 1391.
(63) Ruiz, E.; Cano, J.; Alvarez, S.; Polo, V. *J. Chem. Phys.* **2006**, *124*, 107102.
(64) Ruiz, E.; Cano, J.; Alvarez, S.; Alemany, P. *J. Comput. Chem.* **1999**, *20*, 1391.
(65) Becke, A. D. *J. Chem. Phys.* **1993**, *98*, 5648.
(66) Gräfenstein, J.; Cremer, D. *Theor. Chem. Acc.* **2009**, *123*, 171.
(67) Ruiz, E.; Alvarez, S.; Cano, J.; Polo, V. *J. Chem. Phys.* **2005**, *123*, 164110.
(68) Swart, M. *J. Chem. Theory Comput.* **2008**, *4*, 2057.
(69) Swart, M.; Ehlers, A. W.; Lammertsma, K. *Mol. Phys.* **2004**, *102*, 2467.
(70) Swart, M.; Sola, M.; Bickelhaupt, F. M. *J. Chem. Phys.* **2009**, *131*, 094103.
(71) Ruiz, E. In *Principles and Applications of Density Functional Theory in Inorganic Chemistry II*, 1st ed.; Springer-Verlag: Berlin, 2004; Vol. *113*, p 71.
(72) Ruiz, E.; Alvarez, S.; Rodriguez-Fortea, A.; Alemany, P.; Pouillon, Y.; Massobrio, C. In *Molecules to Materials II: Molecule Based Materials*; Miller, J. S., Drillon, M., Eds.; Wiley-VCH: Weinheim, 2002; Vol. *2*, p 227.
(73) Reiher, M.; Salomon, O.; Hess, B. A. *Theor. Chem. Acc.* **2001**, *107*, 48.
(74) Salomon, O.; Reiher, M.; Hess, B. A. *J. Chem. Phys.* **2002**, *117*, 4729.
(75) Zhao, Y.; Truhlar, D. G. *Theor. Chem. Acc.* **2008**, *120*, 215.
(76) Zhao, Y.; Truhlar, D. G. *Acc. Chem. Res.* **2008**, *41*, 157.
(77) Ruiz, E. *Chem. Phys. Lett.* **2008**, *460*, 336.
(78) Valero, R.; Costa, R.; de P. R. Moreira, I.; Truhlar, D. G.; Illas, F. *J. Chem. Phys.* **2008**, *128*, 114103.
(79) Adamo, C.; Cossi, M.; Scalmani, G.; Barone, V. *Chem. Phys. Lett.* **1999**, *307*, 265.
(80) Jensen, K. P.; Cirera, J. *J. Phys. Chem. A* **2009**, *113*, 10033.
(81) Vancoillie, S.; Zhao, H.; Radoń, M.; Pierloot, K. *J. Chem. Theory Comput.* **2010**, *6*, 576.
(82) Krukau, A. V.; Vydrov, O. A.; Izmaylov, A. F.; Scuseria, G. E. *J. Chem. Phys.* **2006**, *125*, 224106.
(83) Vydrov, O. A.; Scuseria, G. E. *J. Chem. Phys.* **2006**, *125*, 234109.
(84) Peralta, J. E.; Melo, J. I. *J. Chem. Theory Comput.* **2010**, *6*, 1894.
(85) Phillips, J. J.; Peralta, J. E. *J. Chem. Phys.* **2011**, *134*, 034108.
(86) Rivero, P.; de P. R. Moreira, I.; Illas, F.; Scuseria, G. E. *J. Chem. Phys.* **2008**, *129*, 184110.
(87) Yanai, T.; Tew, D. P.; Handy, N. C. *Chem. Phys. Lett.* **2004**, *393*, 51.
(88) Ruiz, E. *J. Comput. Chem.* **2011**, *32*, 1998.
(89) Grimme, S. *J. Chem. Phys.* **2006**, *124*, 034108.
(90) Ye, S.; Neese, F. *Inorg. Chem.* **2010**, *49*, 772.
(91) Schwabe, T.; Grimme, S. *J. Phys. Chem. Lett.* **2010**, *1*, 1201.
(92) Foster, M. E.; Sohlberg, K. *Phys. Chem. Chem. Phys.* **2010**, *12*, 307.
(93) Shao, Y.; Head-Gordon, M.; Krylov, A. I. *J. Chem. Phys.* **2003**, *118*, 4807.
(94) Wang, F.; Ziegler, T. *J. Chem. Phys.* **2004**, *121*, 12191.
(95) Wang, F.; Ziegler, T. *J. Chem. Phys.* **2005**, *122*, 074109.
(96) Wang, F.; Ziegler, T. *Int. J. Quantum Chem.* **2006**, *106*, 2545.
(97) http://www.q-chem.com/.
(98) Valero, R.; Illas, F.; Truhlar, D. G. *J. Chem. Theory Comput.* **2011**, *7*, 3523.
(99) Zhekova, H. R.; Seth, M.; Ziegler, T. *J. Chem. Phys.* **2011**, *135*, 184105.
(100) Zhekova, H.; Seth, M.; Ziegler, T. *J. Chem. Theory Comput.* **2011**, *7*, 1858.
(101) de la Lande, A.; Moliner, V.; Parisel, O. *J. Chem. Phys.* **2007**, *126*, 035102.
(102) Yang, K. *J. Chem. Phys.* **2011**, *135*, 044118.
(103) Baerends, E. J.; Autschbach, J.; Bérces, A.; Bo, C.; Boerrigter, P. M.; Cavallo, L.; Chong, D. P.; Deng, L.; Dickson, R. M.; Ellis, D. E.; van Faassen, M.; Fan, L.; Fischer, T. H.; Guerra, C. F.; van Gisbergen, S. J. A.; Groeneveld, J. A.; Gritsenko, O. V.; Grüning, M.; Harris, F. E.; Hoek, P. v. d.; Jacobsen, H.; Jensen, L.; van Kessel, G.; Kootstra, F.; van Lenthe, E.; McCormack, D. A.; Michalak, A.; Osinga, V. P.; Patchkovskii, S.; Philipsen, P. H. T.; Post, D.; Pye, C. C.; Ravenek, W.; Ros, P.; Schipper, P. R. T.; Schreckenbach, G.; Snijders, J. G.; Sola, M.; Swart, M.; Swerhone, D.; te Velde, G.; Vernooijs, P.; Versluis, L.; Visser, O.; Wang, F.; van Wezenbeek, E.; Wiesenekker, G.; Wolff, S. K.; Woo, T. K.; Yakovlev, A. L.; Ziegler, T. http://www.scm.com, *Scientific Computing and Modelling*.
(104) Frisch, M. J.; Trucks, G. W.; Schlegel, H. B.; Scuseria, G. E.; Robb, M. A.; Cheeseman, J. R.; Scalmani, G.; Barone, V.; Mennucci, B.; Petersson, G. A.; Nakatsuji, H.; Caricato, M.; Li, X.; Hratchian, H. P.; Izmaylov, A. F.; Bloino, J.; Zheng, G.; Sonnenberg, J. L.; Hada, M.; Ehara, M.; Toyota, K.; Fukuda, R.; Hasegawa, J.; Ishida, M.; Nakajima, T.; Honda, Y.; Kitao, O.; Nakai, H.; Vreven, T.; Montgomery, J. A., Jr.; Peralta, J. E.; Ogliaro, F.; Bearpark, M.; Heyd, J. J.; Brothers, E.; Kudin, K. N.; Staroverov, V. N.; Kobayashi, R.; Normand, J.; Raghavachari, K.; Rendell, A.; Burant, J. C.; Iyengar, S. S.; Tomasi, J.; Cossi, M.; Rega, N.; Millam, N. J.; Klene, M.; Knox, J. E.; Cross, J. B.; Bakken, V.; Adamo, C.; Jaramillo, J.; Gomperts, R.; Stratmann, R. E.; Yazyev, O.; Austin, A. J.; Cammi, R.; Pomelli, C.; Ochterski, J. W.; Martin, R. L.; Morokuma, K.; Zakrzewski, V. G.; Voth, G. A.; Salvador, P.; Dannenberg, J. J.; Dapprich, S.; Daniels, A. D.; Farkas, Ö.; Foresman, J. B.; Ortiz, J. V.; Cioslowski, J.; Fox, D. J. *Gaussian09*; 2009.
(105) Seth, M.; Mazur, G.; Ziegler, T. *Theor. Chem. Acc.* **2011**, *129*, 331.
(106) Hirata, S.; Head-Gordon, M. *Chem. Phys. Lett.* **1999**, *314*, 291.

(107) Schafer, A.; Huber, C.; Ahlrichs, R. *J. Chem. Phys.* **1994**, *100*, 5829.
(108) ftp://ftp.chemie.uni-karlsruhe.de/pub/basen/, 2012.
(109) Ciofini, I.; Daul, C. A. *Coord. Chem. Rev.* **2003**, *238*−*239*, 187.
(110) Keal, T. W.; Tozer, D. J. *J. Chem. Phys.* **2003**, *119*, 3015.
(111) Grimme, S. *J. Comput. Chem.* **2006**, *27*, 1787.
(112) Mayer, I. *Int. J. Quantum Chem.* **1986**, *29*, 73.
(113) Bridgeman, A. J.; Cavigliasso, G.; Ireland, L. R.; Rothery, J. *J. Chem. Soc., Dalton Trans.* **2001**, 2095.
(114) Cano, J.; Ruiz, E.; Alvarez, S.; Verdaguer, M. *Comments Inorg. Chem.* **1998**, *20*, 27.
(115) Bertrand, J. A.; Black, T. D.; Eller, P. G.; Helm, F. T.; Mahmood, R. *Inorg. Chem.* **1976**, *15*, 2965.
(116) Bertrand, J. A.; Fujita, E.; VanDerveer, D. G. *Inorg. Chem.* **1980**, *19*, 2022.
(117) Klein, C. L.; Majeste, R. J.; Trefonas, L. M.; O'Connor, C. J. *Inorg. Chem.* **1982**, *21*, 1891.